

Available online at [www.sciencedirect.com](http://www.sciencedirect.com)

**jmr&t**  
Journal of Materials Research and Technology  
[www.jmrt.com.br](http://www.jmrt.com.br)



## Original Article

# Effect of hybrid multi-walled carbon nanotube and montmorillonite nanoclay content on mechanical properties of shape memory epoxy nanocomposite



M.H. Mat Yazik<sup>a</sup>, M.T.H. Sultan<sup>a,b,c,f,\*</sup>, Norkhairunnisa Mazlan<sup>a,b,d</sup>, A. R. Abu Talib<sup>a,d</sup>, J. Naveen<sup>e</sup>, A.U.M. Shah<sup>a,b</sup>, S.N.A. Safri<sup>b</sup>

<sup>a</sup> Department of Aerospace Engineering, Faculty of Engineering, Universiti Putra Malaysia, 43400 UPM Serdang, Selangor Darul Ehsan, Malaysia

<sup>b</sup> Laboratory of Biocomposite Technology, Institute of Tropical Forestry and Forest Products (INTROP), Universiti Putra Malaysia, 43400 UPM Serdang, Selangor Darul Ehsan, Malaysia

<sup>c</sup> Aerospace Malaysia Innovation Centre (944751-A), Prime Minister's Department, MIGHT Partnership Hub, Jalan Impact, 63000 Cyberjaya, Selangor Darul Ehsan, Malaysia

<sup>d</sup> Aerospace Malaysia Research Centre (AMRC), Faculty of Engineering, Universiti Putra Malaysia, Level 7, Tower Block, 43400 UPM Serdang, Selangor, Malaysia

<sup>e</sup> School of Mechanical Engineering, Vellore Institute of Technology, Vellore, 632014, India

<sup>f</sup> UPM Press, Universiti Putra Malaysia, 43400 UPM Serdang, Selangor, Malaysia

## ARTICLE INFO

## Article history:

Received 7 January 2020

Accepted 6 April 2020

Available online 19 April 2020

## Keywords:

Montmorillonite

MWCNT

Hybrid

Shape memory

Nanocomposite

Tensile

Flexural

FESEM.

## ABSTRACT

In this study, the hybrid nanofiller of montmorillonite (MMT) and multi-walled carbon nanotube (MWCNT) were incorporated into shape memory epoxy (SMEP) at different loadings. The fillers were dispersed in the SMEP resin by sonication. Tensile and flexural properties were analyzed at room temperature (RT) and high temperature (HT). Field emission scanning electron microscopy (FE-SEM) was used to analyze the microstructure of fractured samples. The tensile results revealed that at RT, the hybrid filler nanocomposite exhibits a ductile behavior meanwhile at HT, the nanocomposite exhibits a brittle behavior. The sample with the hybrid filler loading of 3 wt% MMT and 1.0 wt% MWCNT produced maximum performance with an increase of 32.5% in the ultimate tensile strength (UTS) and 20.9% in Young's modulus at RT. The trends of the UTS and modulus obtained in the HT tensile test were almost similar to the RT tensile test despite yielding lower value. The RT flexural test revealed an increasing flexural strength as the filler loading increased with a maximum of 176% increase for hybrid filler of 3 wt% MMT and 1.0 wt% MWCNT. This trend was also observed for the flexural strength at HT. From FE-SEM, it was observed that the SMEP nanocomposite containing 3 wt% MMT and 1.0 wt% MWCNT was well dispersed and

\* Corresponding author.

E-mail: [thariq@upm.edu.my](mailto:thariq@upm.edu.my) (M. Sultan).<https://doi.org/10.1016/j.jmrt.2020.04.012>2238-7854/© 2020 The Author(s). Published by Elsevier B.V. This is an open access article under the CC BY-NC-ND license (<http://creativecommons.org/licenses/by-nc-nd/4.0/>).

interact with each other, producing a synergetic reinforcement towards the performance. This study demonstrates the tensile and flexural reinforcement effect of MMT and MWCNT hybrid nanofiller. Findings from this study can be utilized to select the optimum loading for mechanical requirements in various applications.

© 2020 The Author(s). Published by Elsevier B.V. This is an open access article under the CC BY-NC-ND license (<http://creativecommons.org/licenses/by-nc-nd/4.0/>).

## 1. Introduction

Shape memory polymers (SMP) have the ability to be “fixed” at temporary shapes and to recover their “stored” permanent shape upon reaction to certain stimuli [1,2]. In contrast to shape memory alloy such as nickel-titanium alloy, SMP possess many advantages such as light weight, flexibility, high elastic deformation, high shape recovery, and low recovery temperature. The rapid development of SMP in the last decade is attributed to its low manufacturing cost, effortless fabrication processing, excellent structural versatility, and high potential in various industrial applications [3,4]. These advantageous characteristics enable SMP to be used in countless fields and industries including clothing, space structures [5,6], morphing aircraft [7], medical devices [8], and many other applications [9].

Shape memory effect (SME) in polymer is not an elemental property and is often induced by external stimuli such as heat [10], electricity [11], magnetic field [12], light [13], microwave [14], or solution [15]. To date, the most utilized method of actuation is thermally induced SMP, which is mostly triggered by heat [16–22]. Thus far, several types of polymers such as polyethylene [23], polyurethane [24], ethylene-vinyl [25], polystyrene [26–28], poly(ether esters) [29,30], and acrylates [31] have been reported to possess shape memory properties in various applications. Recently, shape memory epoxy polymer (SMEP) has attracted the research community [32–34] because of a few compelling properties such as excellent thermal stability, good processing ability, superior mechanical properties, and high shape fixity and recovery as well as fast recovery response. Interestingly, the thermomechanical properties of SMEP can be adjusted in a large order by varying the formulation [35–40]. Despite its numerous advantages, there are some major limitations of SMP properties that pose great challenges to its extensive utilization [41]. Traditional epoxy matrix resins are mostly brittle in nature, have relatively low strain at break, low cycle durability, and lack of functionalities. Thus, SMP composites are extensively studied to improve the properties of SMEP in order to meet the requirements for commercial applications [42,43].

Reinforcements are commonly accomplished through the incorporation of fillers or fibers into the epoxy matrix. Nanofillers have gained more attention due to its higher surface contact compared to fibrous type reinforcements and conventional fillers. The property improvements of nanofillers have exceeded the achievements of pure epoxy or epoxy composite with macro filler. Moreover, only a small amount of nanofillers are required to obtain improved properties. Nanoparticles with excellent mechanical properties can significantly reinforce nanocomposite with a minimal amount

of 0.006 wt% [44]. Additionally, the incorporation of functional fillers not only enhances the properties of SMEP, but also activates additional triggering methods [45] such as electrical, microwave [14], light [46], and water [47].

Out of many nanofillers that have been studied, carbon nanotube (CNT) has been extensively utilized due to its excellent mechanical, thermal, and electrical properties [48–50]. Since the discovery of multi-walled CNT (MWCNT) by Iijima [51] and the single-walled CNT (SWCNT) [52], the interest in CNT nanocomposite skyrocketed. CNT has been used in various application such as including aerospace, semi-conductor, automotive and remote sensor. The inclusion of CNT in polymer matrix give rise to unique properties such as enhanced electrical properties [53], light sensing [54,55] and electromagnetic absorption [56]. CNT can be found in various structural forms. SWCNT consists of a single layer graphene that is in a cylindrical shape while MWCNT consists of more than two layers of graphene sheet forming a concentric tube either separately, which is mostly capped at the end, or continuously form a single sheet of graphene. MWCNT is easily obtained due to its stable structure and low manufacturing cost, making it the common choice of selection. By the virtue of its high aspect ratio and excellent properties, only a small amount of MWCNT could improve the mechanical properties of SMEP without significantly affecting the shape memory properties of SMEP. A mechanical threshold which in the minimum amount to be added for improved polymer/CNT nanocomposite was estimated to be as low as 0.001 wt% [57].

Arguably the most researched natural product, nanoclay can be obtained in large amounts at a low cost. The large surface area and strong adsorption provides a variety of benefits to epoxy polymers such as enhancing mechanical properties, thermal stability, and barrier properties [58–60]. Typical types of nanoclay are montmorillonite (MMT), hectorite, mica, and bentonite; however montmorillonite is the most widely used nanoclay for various applications. Nanoclays were first reported in the 90s as “hybrid” materials instead of nanocomposite when Usuki et al. [61] and Okada et al. [62] published their work on polyamide-6 filled with nanoclay, which interestingly kick-started the method of incorporating nanofillers into the polymer matrix as reinforcements.

The simultaneous presence of MWCNT and MMT in the polymer matrix could provide the advantages of both types of nanofillers and activate a multifunctional material. The interaction of hybrid nanoparticles in 3D hierarchical hybrid structures consisting of various 1D and 2D nanoparticles can be illustrated through the schematic diagram in Fig. 1.

Figure 1a) shows a phase-separated composite where the fillers stay in the same range as the traditional micro-composite. Fig. 1b) shows disordered and loose fillers in the

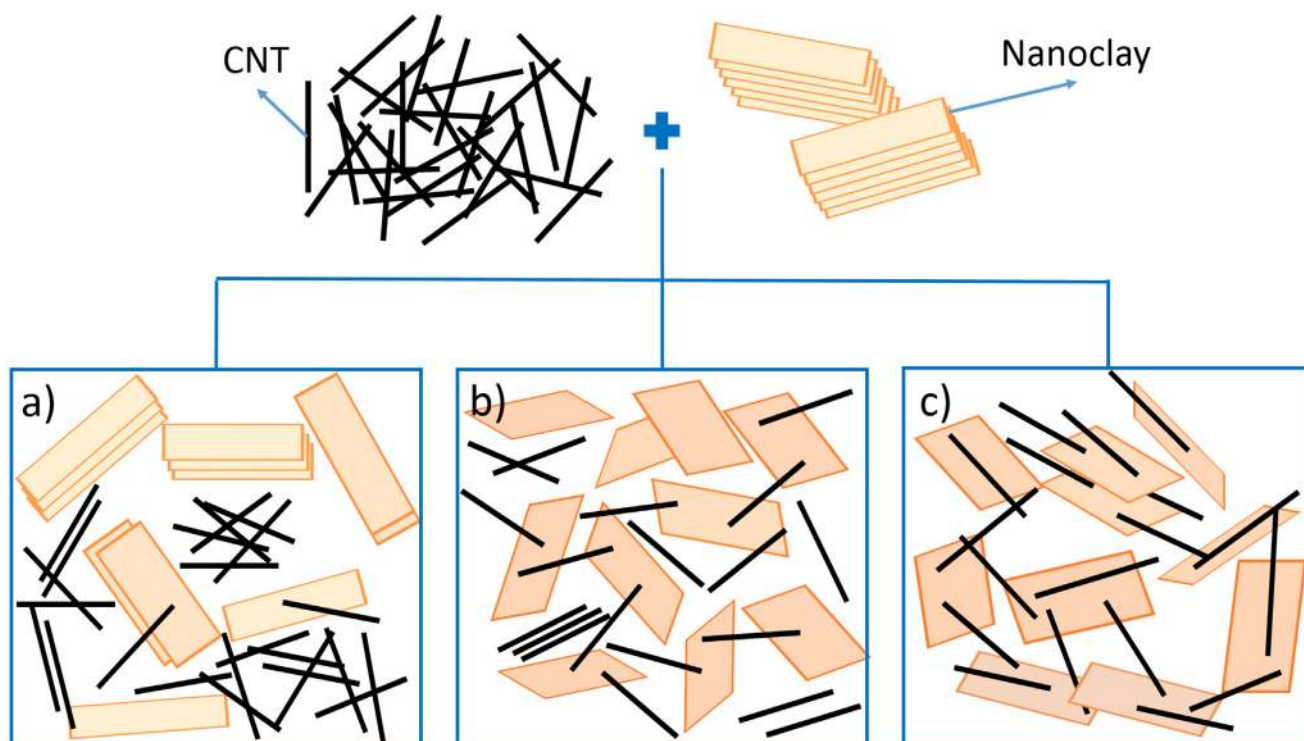


Fig. 1 – 3D structures consisting of 1D Nanoclay and 2D Carbon Nanotube nanomaterials.

polymer matrix where some of the CNT and nanoclays did not take part in the formation of the hybrid network due to the lack of interaction between them. This interaction is mostly a point-to-point contact. Meanwhile, Fig. 1c) shows a compact formation of nanofillers in which these fillers are connected through face-to-face contact through strong  $\pi$ - $\pi$  interaction [63]. The dispersion of nanofillers in the polymeric matrix in order to obtain the exfoliated nanofiller remains one of the difficulties in producing nanocomposite. Zare found that the distance between nanoparticles and polymer changes affected the tensile strength of interphase layer by a power function [64]. When the filler size is analogous to polymer chain, the interaction between nanoparticle and polymer matrix at atomic scale produce a third phase between them called the interphase. The properties of interphase determine the stress transfer from the polymer to the nanoparticles and thus affecting the mechanical properties [65]. Although various studies have been done on the effect of infusing either MWCNT or MMT into the polymer matrix, the effect of the hybrid presence of both nanofillers are rarely reported especially on SMEP matrix. These limited studies have shown disparity in the number of optimal percentage loading to maximize the improvement in mechanical properties. Other than that, interface region also plays an important role in determining the mechanical properties of nanocomposite.

Sun et al. studied the effect of CNT loading using nanoclay-like filler as a dispersion agent for CNT via strong electrostatic affinity between those two fillers and found that a low CNT content results in increasing modulus, strength, and strain at failure [66]. On the other hand, Zhao et al. used clay-supported CNT to improve the thermal and mechanical properties of

poly (vinyl alcohol) [67]. The study showed that the thermal and mechanical properties of the polymer were enhanced by the incorporation of the nanofillers. Meanwhile, Kim et al. used functionalized clay and MWCNT to reinforce the electrical and mechanical properties of poly (L-lactide) [68] and reported an improvement in the mechanical properties for the hybrid nanocomposite as compared to pure resin. Ayatollahi et al. conducted a research on the effects of MWCNT and nanoclay on the mechanical properties of epoxy nanocomposite [69]. They reported that different nanofiller content produced various modification to the mechanical properties and that 0.5% MWCNT produced the maximum improvement over neat epoxy.

A more recent study by Mehmet et al. on the mechanical properties of individual CNT and nanoclay nanocomposite as well as the hybrid nanocomposite in epoxy showed a lower improvement in flexural compared to the individual filler nanocomposites [70]. They concluded that the amount of nanofiller used was excessive and that the effect of the filler loading need to be studied to maximize the hybridization reinforcement effect. Per contra, Hosur et al. showed that the improvement in terms of the mechanical and thermomechanical properties of hybrid CNT and MMT nanocomposite was higher than that of the individual filler nanocomposite at a low hybrid filler content [71]. In another study, similar findings were obtained by Zeng et al. at lower hybrid filler content [72]. However, only a few researchers studied the effects of different MWCNT and MMT filler contents on the mechanical properties of epoxy polymer.

In this study, the presence of hybrid MMT and MWCNT at different filler loadings are studied in relation to the mechan-

ical properties of the resulting hybrid SMEP nanocomposites. Firstly, the hybrid nanocomposite were prepared by dispersing the MMT and MWCNT with ultra-sonication into the epoxy solution. Then, the mechanical behavior of the fabricated nanocomposite were evaluated through a series of tensile and flexural tests at different temperature values above and below its  $T_g$  ( $\sim 56^\circ\text{C}$ ). Finally, we present the synergetic effect of MMT and MWCNT through the morphological analysis of the tensile fracture surface of the nanocomposites.

## 2. Materials and method

### 2.1. Materials

The materials used to fabricate the shape memory polymer consist of a hard and a soft segment epoxy. Diglycidyl ether bisphenol-A aromatic diepoxide monomer, EPON 826 was used as the hard segment while aliphatic diepoxide, Neopentyl glycol diglycidyl ether (NGDE) as the soft segment. The materials were obtained from Hexion (Germany) and TCI America (USA), respectively. The curing agent used were poly(propylene glycol)bis(2-aminopropyl)ether (Jeffamine D230) obtained from Huntsman (USA). The chemical structures of the SMEP matrix formulation are shown in Fig. 2.

The SME are obtained due to the difference in the chemical structure of both the hard and soft segments of the epoxies. The curing agent used in this formulation contain an amine group,  $-\text{NH}_2$ , which reacts with both the segments to create a crosslink between the epoxies. The connection occurs at a net-point which can be attached to either EPON 826 or NGDE end chain [73]. Nanomer I.31PS is a Montmorillonite (MMT) clay modified with 15–35% octyadecylamine and 0.5–5% aminopropyl triethoxysilane obtained from Sigma-Aldrich Chemistry (USA). MMT are originally hydrophilic due to the presence of counter-ions  $\text{Na}^+$  and  $\text{Ca}^{2+}$  on the surface, resulting in a difficulty to disperse in the epoxy polymer matrix [74]. Through surface modification, the counter-ions are replaced with organic cations which makes it hydrophobic, thus, compatible with the epoxy matrix. MWCNT used in this study was obtained from ZKK Sdn Bhd (Malaysia). MWCNT produced by the carbon vapor deposition (CVD) process produced high purity (more than 97%) containing 8–15 nanotube layers with diameters and length in the range of 12 nm–15 nm and 3  $\mu\text{m}$ –15  $\mu\text{m}$ , respectively.

### 2.2. Sample preparation

In order to examine the effect of the nanofiller addition to SMEP, both neat SMEP and hybrid SMEP were fabricated according to the following procedure. The details of the SMEP matrix formulation were obtained from Table 1 in Xie and Rousseau [36]. EPON826, NGDE, and Jeffamine D230 were weighed according to the prescribed molar ratio of 0.0:1:0.01:0.01. EPON826 was heated at  $60^\circ\text{C}$  for 10 min before being gradually mixed with the other two solutions. The mixtures were hand-stirred for 5 min until a clear mixture was obtained. Then, the mixture was poured in an aluminum mold with a dimension of 300 mm  $\times$  300 mm and was put under a vacuum condition with a pressure of 100 kPa at  $65^\circ\text{C}$  for 30 min

**Table 1 – Hybrid nanocomposite label according to nanofiller content.**

Label	MMT %, (wt %)	MWCNT %, (wt %)
NEAT	0	0
1MT 0.5NT	1	0.5
1MT 1.0NT	1	1.0
1MT 1.5NT	1	1.5
3MT 0.5NT	3	0.5
3MT 1.0NT	3	1.0
3MT 1.5NT	3	1.5
5MT 0.5NT	5	0.5
5MT 1.0NT	5	1.0
5MT 1.5NT	5	1.5

to remove any bubble formed in the mixture. The mixture was then pre-cured in isothermal stepwise manner to prevent bubble formation in which the temperature was raised  $10^\circ\text{C}$  and maintained for 5 min until it reached  $100^\circ\text{C}$ . Then, it was cured at  $100^\circ\text{C}$  for 1.5 h and subsequently post-cured at  $130^\circ\text{C}$  for 1 h.

The fabrication of hybrid nanocomposite was conducted as follows. Initially, MMT were dried in a thermal oven at  $100^\circ\text{C}$  for 24 h. Then, the nanofillers were weighed precisely using a weighing machine according to the weight percentage of the final matrix mixture. The amounts used for MMT were 1%, 3%, and 5% weight percentage of the mixture. Meanwhile, the amounts of MWCNT used were 0.5%, 1.0%, and 1.5% weight percentage of the mixture. Then, the nanofillers were added into the pre-weighed Jeffamine D230 solution. The curing agent was used as the dispersing medium to obtain a better dispersion as indicated in a previous study [75]. The solution of nanofillers and Jeffamine D230 were hand-stirred to disperse the nanofillers. The mixture was then sonicated using a 650 W ultrasonic cell crushed noise isolating chamber at 50% amplitude with 3.0 s start time and 1.0 s pause time. The remaining procedures were the same as the procedures conducted for neat SMEP. Fig. 3 shows the fabrication flow of the hybrid MWCNT/Nanoclay SMEP. In the discussion section, the hybrid filler SMEP was labelled according to its filler content combination as shown in Table 1 below.

### 2.3. Characterization

#### 2.3.1. Tensile test

Tensile test was conducted at two different temperatures: below  $T_g$  at room temperature (RT) around  $25^\circ\text{C}$  and at a high temperature (HT) well above  $T_g$  around  $80^\circ\text{C}$ . The samples were cut from the plate using water jet cutting into a dumbbell shape according to ASTM D638 type V dimension [76]. For the RT tensile test, the INSTRON 5567 Universal Testing Machine with a 30 kN load capacity was used. Meanwhile, for the HT tensile test, the SHIMADZU AG-X plus Universal Testing Machine with a 20 kN load capacity was used fitted with the SHIMADZU TCE-N300-CE Thermostatic Chamber to control the temperature at  $80 \pm 1.5^\circ\text{C}$ . Both tests were conducted at a crosshead speed of 1 mm/min. Five samples were tested for each hybrid combination and the most representative curve was plotted for analysis. The load and extension

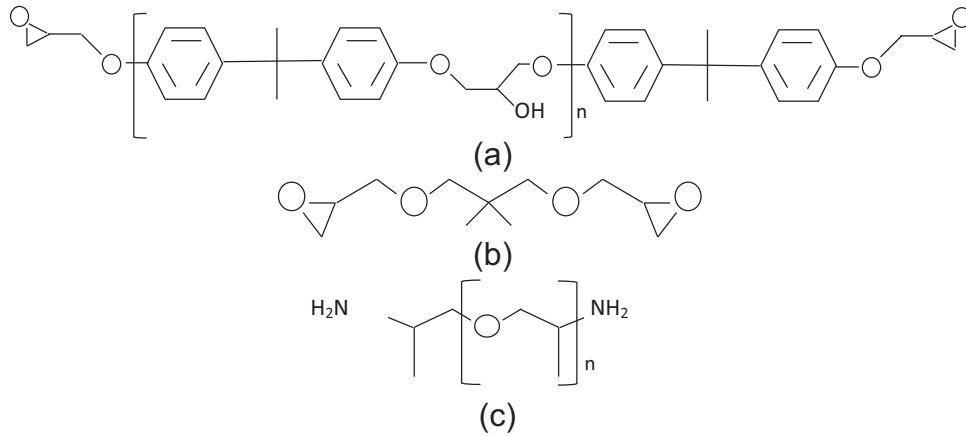


Fig. 2 – Chemical structure of SMEP matrix formulation [35,73]: (a) EPON 826, where n = 0.085; (b) Neopentyl glycol diglycidyl ether (NGDE); (c) Jeffamine D-230 where n = 2.5.

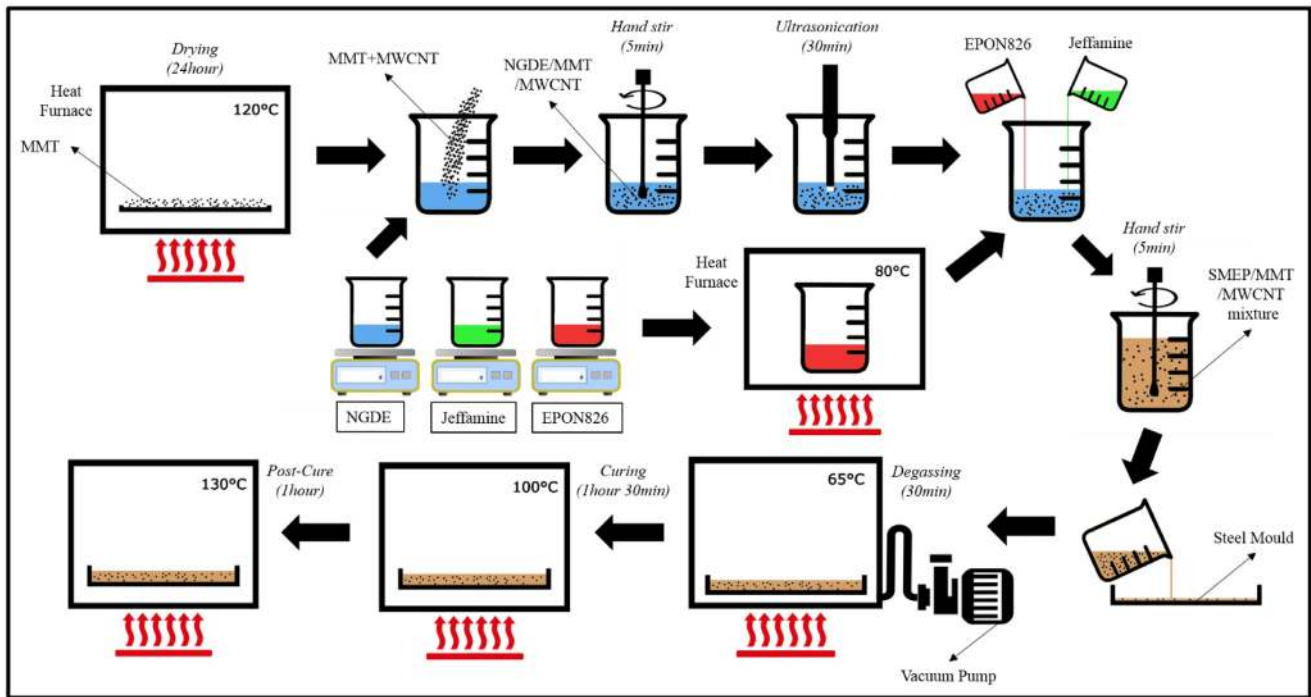


Fig. 3 – Fabrication of Hybrid MWCNT/Nanoclay SMEP.

response were recorded while the stress,  $\sigma$ , and strain,  $\epsilon$ , were calculated using the following equations;

$$\sigma_t = \frac{F}{A} \quad (1)$$

$$\epsilon_t = \frac{e}{L} \quad (2)$$

where  $F$  the load is applied in Newton and  $A$  is the minimum cross sectional area of the sample in  $mm^2$  while  $e$  is the extension of upon loading and  $L$  is the initial length, both in  $mm$ .

### 2.3.2. Flexural test

Flexural test was also conducted at two different temperatures at 25 °C (RT) and 80 °C (HT). The samples were cut from the plate using water jet cutting according to ASTM D790 with the recommended span-to-depth ratio of 16:1 [77]. The RT flexural test was conducted using the INSTRON 5567 Universal Testing Machine with a 30 kN load capacity. Meanwhile, the HT flexural test was conducted using the INSTRON 5509 Universal Testing Machine with a 20 kN load capacity with the INSTRON 3119–407 Environmental Chamber for temperature control at  $80 \pm 3$  °C. At least five specimens were tested for each hybrid combination. The tests were conducted with a crosshead speed of 16.67 mm/min until 20% strain elongation was achieved or until the specimen started to slip from the

clamp, whichever comes first. The force and deflection data was recorded, and a representative curve was plotted. The load and extension response were recorded, and the stress,  $\sigma$ , and strain,  $\varepsilon$ , were calculated using the following equations;

$$\sigma_f = \frac{3FL}{2bd^2} \quad (3)$$

$$\varepsilon_f = \frac{6ed}{L^2} \quad (4)$$

where  $F$  is the load applied in Newton,  $L$  is the support span in  $mm$ ,  $b$  and  $d$  were width and thickness of the sample respectively, both in  $mm$  while  $e$  is the deflection of beam, in  $mm$ .

### 2.3.3. Field emission scanning Electron microscopy (FESEM)

FESEM was used to evaluate the characteristics of the fractured surface. Nova NanoSEM 30 Series from FEI Company was used to evaluate the dispersion level of MWCNT and MMT hybrid in the epoxy matrix of SMEP nanocomposites. The fractured surfaces were examined at 10 kV accelerating voltage and coated in gold particle prior to SEM in order to make the organic material electron conducting thus reducing the electrostatic charge generated when the electron beam hit the material.

## 3. Results and discussion

### 3.1. Tensile properties

The tensile test is a destructive test process that supplies the mechanical information about the tensile strength, yield strength, and ductility of materials. The test measures the force required to break the materials to the extent where the specimen stretches or extends to the breaking point [78]. The stress-strain curve of a tensile test is usually analyzed to obtain the ultimate tensile strength and the elongation strain at its breaking point as well as calculating the tensile modulus, known as Young's modulus. Composites are commonly anisotropic materials which display different tensile properties in different axis. Assuming a well dispersed nanoparticle in the nanocomposite, the materials are considered as anisotropic material. Most plastics will show one of four basic types of materials: brittle, stiff and strong, stiff and tough, and soft materials as indicated by their stress-strain curve [79]. The tensile modulus is a measure of flexibility in the axis of strain measurement. It is measured along the linear-elastic region of the stress-strain curve by dividing the force distributed over the samples' cross-sectional area and the relative change in the length over the initial length.

#### 3.1.1. Room temperature

Fig. 4 above shows the stress-strain curve of the SMEP and hybrid SMEP nanocomposite calculated from Eq.s (1) and (2). Initial observation in Fig. 4 (a)-(c) shows that the material exhibited a stiff and strong behavior. The tensile curves of all samples showed a similar trend, which can be divided into three parts. The first part is a quasi-linear response towards the load where the stress increased as the strain increased. The second stage is a non-linear response where the curve

peaked at a maximum value, known as the ultimate tensile strength (UTS) and beyond that point, the stress decreased as the strain increased. The third part is where the materials started to flow shown by the decays in the stress to a plateau before the sample breaks.

The ultimate tensile strength (UTS) of Neat SMEP was recorded at 34.3 MPa. The lowest UTS was obtained by 3 MT 0.5 NT at 26.07 MPa (a decrease by 23.9%) while the highest was 3 MT 1.0 NT at 45.47 MPa (an increase by 32.5%). For the low filler content, i.e., 0.5 wt% MMT, the increase in MWCNT content saw an increase in the UTS. This can be attributed to the reinforcing effect of MMT and MWCNT in the nanocomposite. The high surface area of nanofiller provides a more efficient stress transfer to the filler, thus strengthening the materials. This correlate with the model developed in [80] where low filler content produces lowest tensile strength independent of the interphase properties. For the hybrid filler SMEP with 3 wt% MMT, the inclusion of 1.0 wt% MWCNT resulted in the highest UTS compared to 0.5 wt% and 1.5 wt% MWCNT. This is probably due to the agglomeration that occurred at high filler content. The amount of filler in 3 MT 1.5 NT nanocomposite reached the threshold amount for the effective reinforcement of the hybrid nanofiller. A poor interfacial adhesion is obtained between polymer and nanofiller which cause aggregation and produce nanocomposite with lower tensile strength as predicted in [80]. This produced lumps or clusters of nanofillers which were held by strong Van der Walls force [81] and prevented the wetting of the nanofiller by epoxy, thus disabling the stress transfer to the nanofiller. This led to a stress concentration area which is highly susceptible to material failure at the same area. Similar observations were reported in a previous study [82].

On the other hand, the variation of the tensile strength of hybrid SMEP with 5 wt% MMT showed a reverse trend from those with 3 wt% of MMT. This behavior was unexpected and probably caused by the uneven dispersion of nanofillers in the SMEP matrix. The uneven dispersion is caused by the agglomeration where the materials appear as non-homogenous and exist in a two-phase system: the matrix phase and the nanofiller phase [83]. Fig. 4 (d) shows the obtained modulus for the hybrid SMEP nanocomposite varied with the nanofiller contents. The Young's modulus of Neat SMEP was calculated as 7.43 GPa. The trend of Young's modulus followed the corresponding UTS trend which saw 3 MT 1.0 NT recording the highest Young's Modulus among the nanocomposites at about 9.0 GPa which translated to an increase of approximately 20.9% from Neat SMEP. Meanwhile, the lowest Young's modulus was recorded by 3 MT 0.5 NT at 6.22 GPa which corresponds to approximately 16.2% decrease compared to Neat SMEP.

#### 3.1.2. High temperature

Fig. 5 shows the stress-strain curve calculated according to Eq.s (1) and (2). Graph in Fig. 5 (a)-(c), clearly show a brittle behavior of the material at 80 °C. The increase in the strain showed a corresponding increase in the stress up to the failure point. However, note that the stress was significantly lower than the test conducted at the lower temperature. This is due to the material transition from the glassy state to the rubbery state when exposed to a temperature above  $T_g$ , leading to a drastic drop in the modulus [84]. The change of modu-

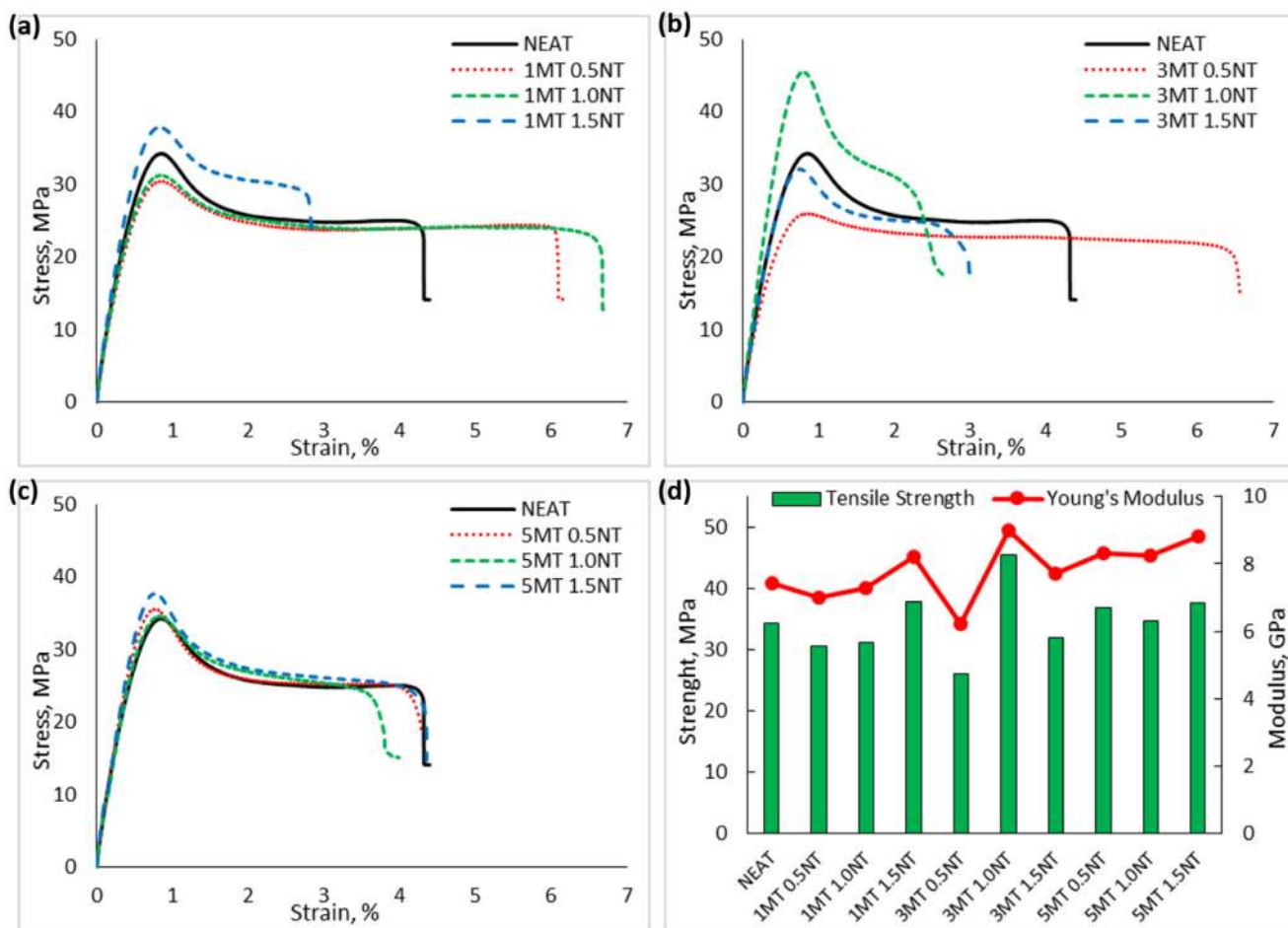


**Fig. 4 – RT tensile response of SMEP and hybrid MMT/MWCNT SMEP nanocomposite (a) Variation of Stress-Strain curve for hybrid SMEP with 1% MMT (b) Variation of Stress-Strain curve for hybrid SMEP with 3% MMT (c) Variation of Stress-Strain curve of hybrid SMEP with 5% MMT (d) UTS and Young's Modulus of SMEP and hybrid SMEP nanocomposites.**

lus for each material was more than two order of magnitude compared to its properties at room temperature. The trend of Young's modulus obtained at high temperature was almost similar to the modulus at room temperature. This shows that the change in modulus is primarily due to the change in material properties and does not significantly affect the reinforcing effect of the hybrid nanofillers. However, the trend in the UTS for hybrid SMEP with 5% MMT shows a different behavior than the tensile test at RT. This is probably due to the high concentration of nanofiller which increased the extent of anisotropy in the polymer producing various properties [85]. As compared to the tensile test at RT in Fig. 4 (d), the increase in the strength of the hybrid nanocomposite for 5% MMT shows that the reinforcement effect of hybrid MMT and MWCNT were enhanced at an elevated temperature. From Fig. 5 (d), we can see that the UTS of the hybrid filler SMEP at an elevated temperature behaved differently compared to the behavior at room temperatures. The corresponding stress was significantly less than that observed in the room temperature tensile test. The UTS for Neat SMEP was 1.209 MPa with a Young's Modulus of 0.039 GPa. The highest UTS was obtained by 3 MT 1.0 NT at 1.811 MPa, approximately 49% increase compared to Neat

SMEP, while the lowest was 3 MT 0.5 NT at 1.363 MPa, corresponding to an improvement of 12%. This implies that only a small force was required to deform the SMEP at an elevated temperature.

Note that the materials exhibited a larger elongation at break compared to the tensile test at room temperature. This is because above  $T_g$ , the micro Brownian movement of polymeric chain reduced the modulus, thus increasing the molecular mobility [86]. Hence, the tightly packed structures of rigid polymer loses its packed arrangement and deforms easily. The elongation might also be caused by the evolution of the linkage state of the matrix [87]. Post-curing of the SMEP matrix may have occurred at this temperature prior to the decomposition process. A minor softening of the matrix might occur at this temperature enabling the resin to penetrate the nanofiller and reducing the void content inside the matrix [88]. These properties are suitable for applications such as morphing structures or biomedical sutures which prefer lower shaping force to shape the materials [2,89,90]. However, a significant consideration is required to ensure that the materials do not reach its breaking point as the materials exhibit brittle failure and do not show any yielding before break at an elevated temperature.

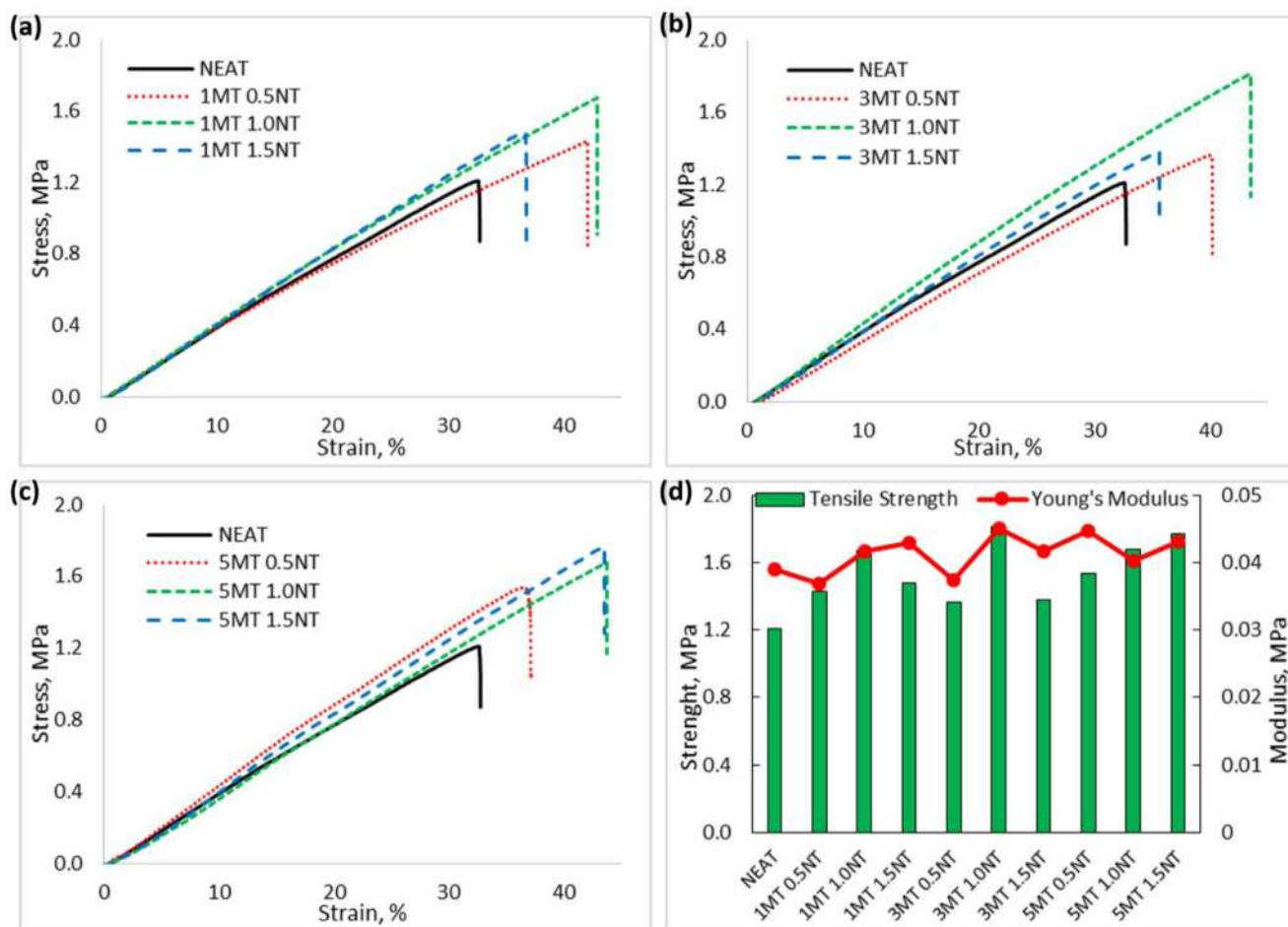


**Fig. 5 – HT tensile response of SMEP and hybrid MMT/MWCNT SMEP nanocomposite showing brittle properties (a) Variation of Stress-Strain curve for hybrid SMEP with 1% MMT (b) Variation of Stress-Strain curve for hybrid SMEP with 3% MMT (c) Variation of Stress-Strain curve of hybrid SMEP with 5% MMT (d) UTS and Young's Modulus of SMEP and hybrid SMEP nanocomposites.**

### 3.2. Flexural properties

Flexural test measures the force required to bend a beam of materials and determine the stiffness of a material. The stress-strain curve are obtained to measure the flexural strength and flexural modulus. Flexural test is generally applicable for both rigid and semi-rigid materials, either resin or laminated composite materials [78,91]. During bending, the surface where load is applied experiences a compressive force while the surface opposite of the applied load experiences a tensile force. Flexural modulus is a measure of stiffness to bending when a force is applied perpendicular to the sample in a three-point bending test. Similar to the tensile modulus, this is measured along the linear-elastic region of the stress-strain curve.

#### 3.2.1. Room temperature

The behavior of SMEP and hybrid filler SMEP nanocomposite upon flexural test at RT are shown in Fig. 6. Note that the sample tested did not yield during the tests, owing to the nanocomposite's ability to withstand a large enough deflection that it slipped off the anvil before yielding. In the instance

that this situation occurred, the test was halted. The load and displacement data were recorded, and the stress-strain was calculated according to Eq.s (3) and (4). The general analysis of the stress-strain curve shows an initial elastic response followed by a plateau akin to a perfectly plastic response. Analogous response was recorded for the SMEP and hybrid filler SMEP nanocomposites. The ultimate flexural strength was defined as the maximum stress in its respective stress-strain curve. The flexural strength of Neat SMEP was recorded at 26.53 MPa with a modulus of 1.12 GPa. From Fig. 6 (a)-(c), it can be seen that all the hybrid SMEP nanocomposites performed better than Neat SMEP with its properties varying depending on its filler content.

For the hybrid filler with 1 wt% MMT, there was an increase in the flexural strength as the content of MWCNT increased. The increase in the flexural strength can be explained by the incorporation of higher dispersed MWCNT inside the SMEP matrix which inhibits the mobility of the polymer chain under flexural load [92]. The highest flexural strength was obtained with hybridization of 3 wt% MMT and 1.0 wt% MWCNT into the SMEP matrix at 73.41 MPa. This rendered an increase of 176% in the flexural strength compared to Neat SMEP.

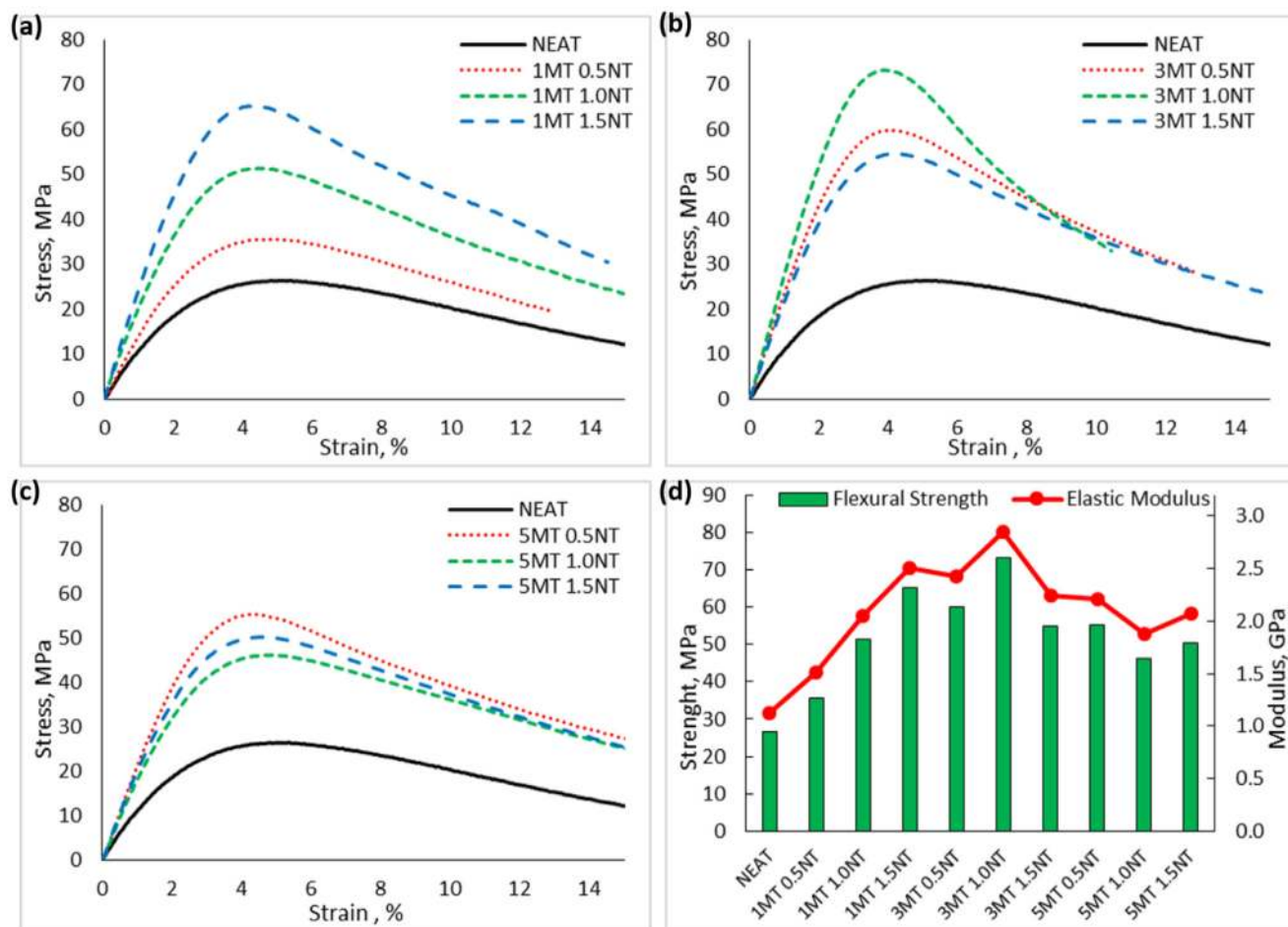


**Fig. 6 – RT flexural behavior of SMEP and hybrid MMT/MWCNT SMEP nanocomposites (a) Variation of Stress-Strain curve for hybrid SMEP with 1% MMT (b) Variation of Stress-Strain curve for hybrid SMEP with 3% MMT (c) Variation of Stress-Strain curve of hybrid SMEP with 5% MMT (d) UTS and Young's Modulus of SMEP and hybrid SMEP nanocomposites.**

The performance is devoted to the fact that the dispersion of MMT and MWCNT in the SMEP matrix was better than other hybrid nanocomposites. As established in the literature, the high aspect ratio of MWCNT was among the crucial factors to improve the flexural strength [93]. On the other hand, the aspect ratio of MMT also affects the strength of nanocomposite according to a model developed in [94]. This model describes a proportional relation between MMT aspect ratio and strength of nanocomposite. A high aspect ratio indicates a good extent of intercalation/exfoliation of MMT platelets in nanocomposite. The uniform dispersion of MMT and MWCNT filler provided a uniform distribution of stress and reduced the sites of stress concentrations in the SMEP matrix. The comparison of the flexural modulus is plotted in Fig. 6 (d). For the hybrid filler with 1 wt% MMT, the incorporation of 0.5 wt%, 1.0 wt%, and 1.5 wt% MWCNT yielded 1.51 GPa, 2.05 GPa, and 2.51 GPa, respectively. Similarly, for the hybrid filler with 3 wt% MMT, the hybridization with 0.5 wt%, 1.0 wt%, and 1.5 wt% MWCNT yielded 2.43 GPa, 2.85 GPa, and 2.24 GPa, respectively. Meanwhile, the flexural modulus for the hybridization of 5 wt% MMT with 0.5 wt%, 1.0 wt%, and 1.5 wt% MWCNT produced 2.20 GPa, 1.87 GPa, and 2.06 GPa, respectively.

Note the decrease in the flexural strength and modulus for the hybrid filler SMEP with 5 wt% MMT compared to the others. This displeasing discovery can be attributed to the reinforcement efficiency of MMT and MWCNT. The filler content has achieved the percolation threshold where further increase in the filler content would lead to a decreasing reinforcement efficiency [95]. This is caused by the formation of agglomeration and cluster which simulated large particles in the SMEP matrix. The agglomeration reduced the effective surface area of the nanoparticle filler and formed a void space in the matrix and effectively reduced the volume fraction of SMEP matrix [96]. This led to a non-uniform stress transfer and the formation of stress concentration area which resulted in a mechanical failure when subjected to flexural load. Similar behavior was reported in previous studies related to hybrid composite [82,97].

### 3.2.2. High temperature

The flexural response of SMEP and hybrid filler SMEP nanocomposites are shown in Fig. 7. The load and extension data were recorded and analyzed to obtain the stress-strain data. The flexural modulus results for the HT tests are found to be inconclusive. As illustrated in Fig. 7 (a)-(c), a large amount

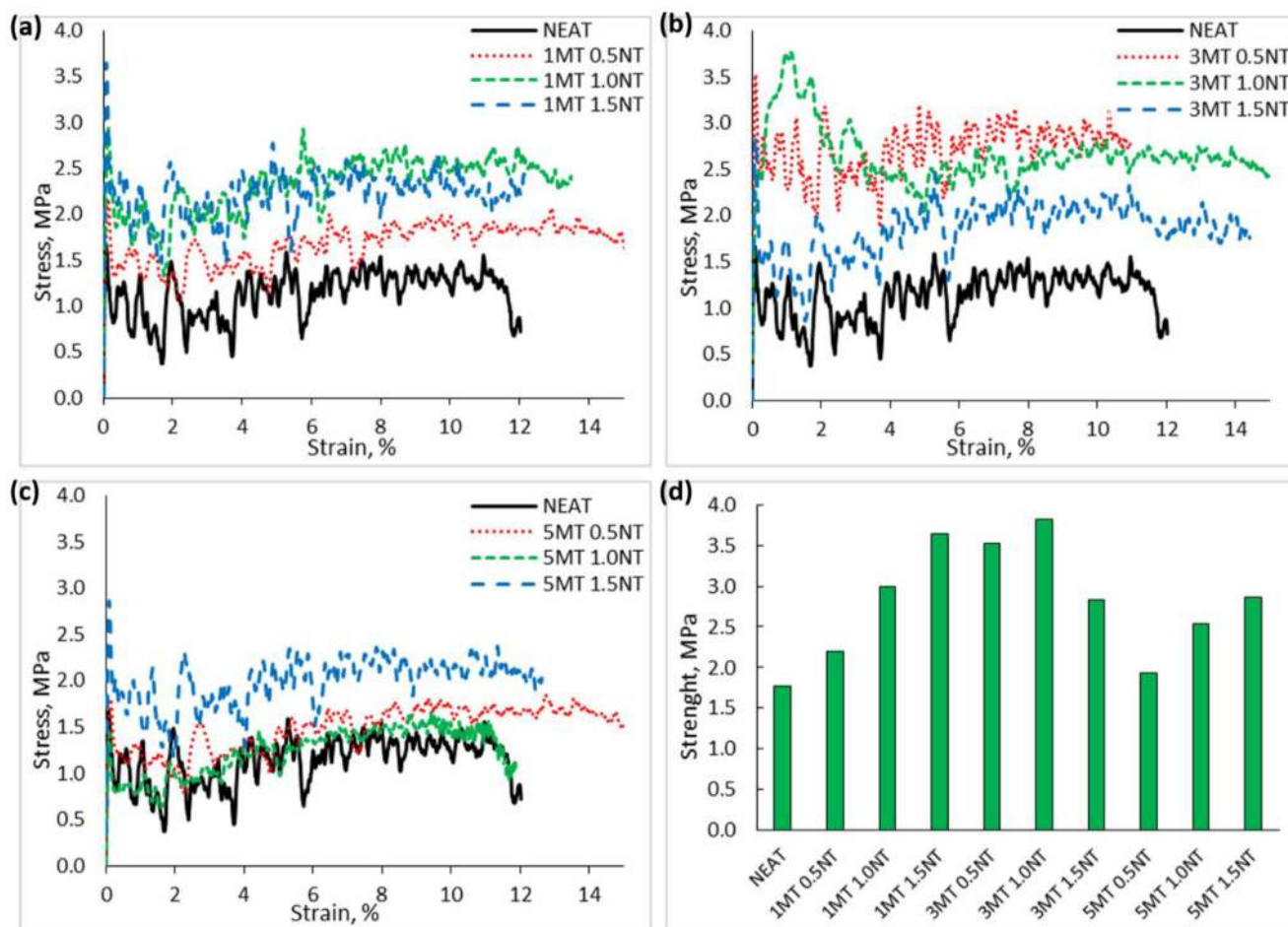


**Fig. 7 – HT flexural response of SMEP and hybrid MMT/MWCNT SMEP nanocomposites. (a) Variation of Stress-Strain curve for hybrid SMEP with 1% MMT (b) Variation of Stress-Strain curve for hybrid SMEP with 3% MMT (c) Variation of Stress-Strain curve of hybrid SMEP with 5% MMT (d) UTS and Young's Modulus of SMEP and hybrid SMEP nanocomposites.**

of scatter were found on the response due to the fact that the load frame employed during these tests was operating at its absolute limit of its resolution when small loads were imposed at an elevated temperature. At each test, the load was applied after the temperature of the sample reached approximately 80 °C to avoid the sample slipping from the anvil. The data acquisition rates were not high enough to give a clear line of the elastic region of the stress-strain curve. Similar behavior was previously reported for flexural test at an elevated temperature [98]. The flexural test, however, clearly indicated the peak flexural stress which are plotted in Fig. 7(d). Note that the maximum flexural stress mostly occurred at the beginning of the test. From the data, it can be seen that the flexural strength reduced drastically compared to the flexural stress at room temperature. The characteristic was predominantly caused by the SMEP matrix which crucially affected the overall performance of the hybrid filler SMEP nanocomposites [99].

Note that the trend of the flexural strength with respect to the filler content at an elevated temperature are almost analogous to the trend obtained at room temperature. From the data collected, the highest flexural strength obtained from the test were recorded by 3 MT 1.0 NT at 3.82 MPa, approximately 114.9% increase from the Neat SMEP which recorded

a peak of 1.76 MPa. This can be attributed to the dispersed distribution of nanofiller in the SMEP matrix. Macromolecular chain plays an important role in resisting mechanical loadings. The motion of the macromolecular chains were hindered by the MMT and MWCNT filler through friction interaction, thus helping the SMEP matrix to resist the flexural loading and ensuring improved mechanical properties [100].

Meanwhile, the lowest increment was recorded by 5 MT 0.5 NT, with approximately 9.29% increment in the flexural strength. As stated above, this is probably caused by the formation of filler cluster and agglomeration which produce a stress concentration area and can subsequently lead to material failure when subjected to flexural loading. However, compared to the RT flexural test, the flexural strength of the hybrid with 5% MMT at HT shows an increasing trend with increasing MWCNT content. This shows that the reinforcement effects of MMT and MWCNT were enhanced at an elevated temperature for the hybrid nanocomposite with 5% MMT content. Similar to the HT tensile test, in HT flexural test, only a small stress was required to produce an equal amount of deformation on the hybrid SMEP nanocomposite. This decrement in the flexural strength can be predominantly related to the loss in rigidity of a tightly packed SMEP structure above its  $T_g$ . The

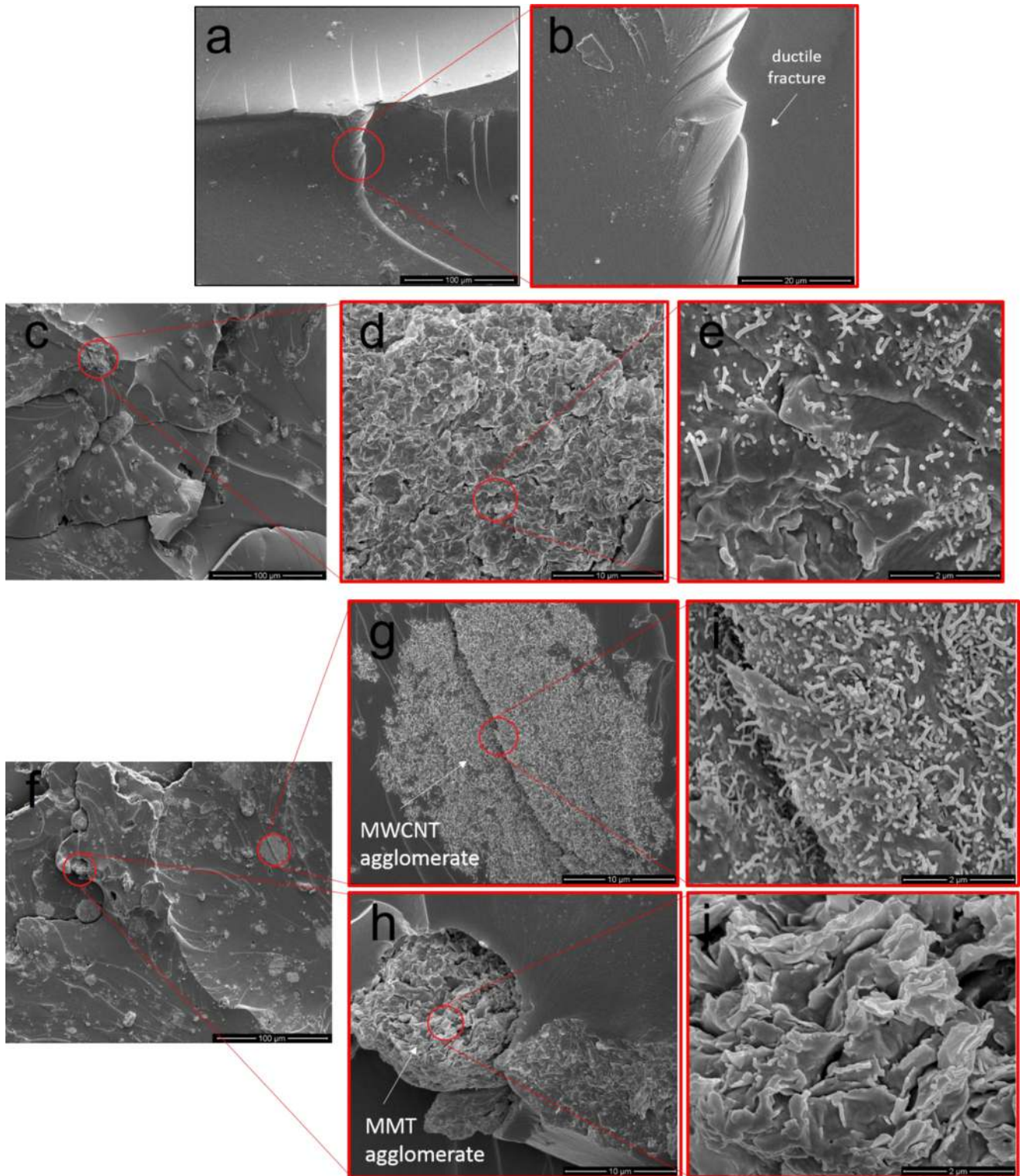


**Fig. 8 – FESEM images of fracture from RT tensile test of Neat SMEP (a) and (b), 3 MT 1.0 NT (c)–(e) and 5 MT 1.0 NT (f)–(j) at different magnification levels. (a), (c), and (f) were taken at low magnification (x1000); (b) was taken at x5000 magnification in the red circle area of (a). (d), (g), and (h) were taken at medium magnification (x10 000) in the red circle area of (c) and (f). While (e), (i), and (j) were taken at high magnification (x50 000) in the red circle area of (d), (g), and (h) respectively.**

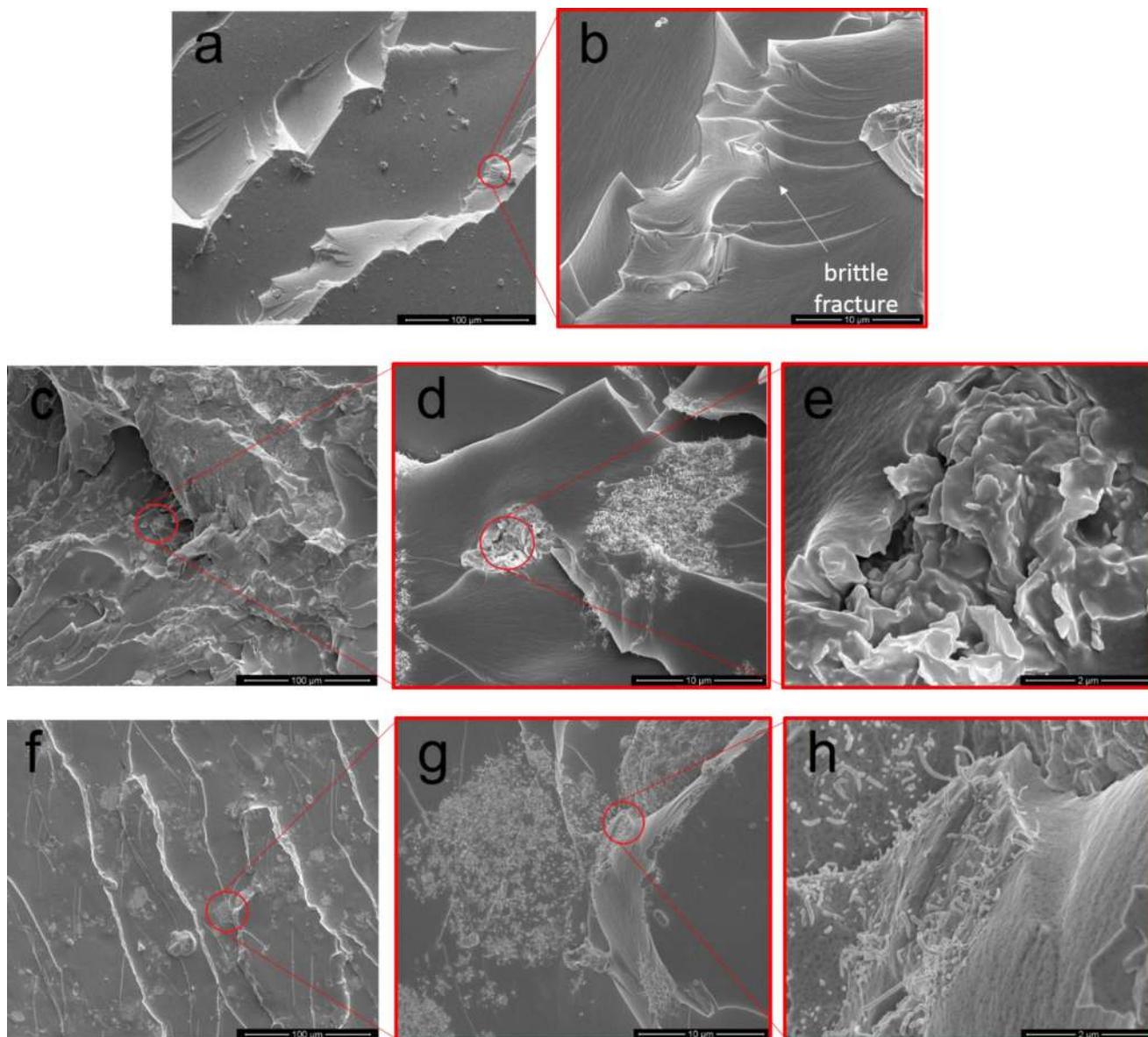


**Fig. 9** – FESEM images of fracture from HT tensile test of Neat SMEP (a) and (b), 1MT 0.5NT (c)–(e) and 3MT 1.0NT (f)–(h) at different magnification levels. (a), (c), and (f) are taken at low magnification (x1000); (b), (d), and (g) are taken at medium magnification (x10 000) in red circle area of (a), (c), and (f) respectively; while (e) and (h) are taken at high magnification (x50 000) in red circle area of (b), (d), and (g) respectively.

SMEP matrix softens and can be easily deformed due to the increase in chain movement in the matrix.

### 3.3. Morphological analysis

The efficiency of MMT and MWCNT as the hybrid nanofiller in SMEP matrix is fundamentally determined by the degree of dispersion in the matrix as well as the interaction and interfacial bonding with the matrix. Therefore, morphological analysis is crucial for the determination of the dispersion and interaction of the nanofiller and SMEP matrix.

#### 3.3.1. Room temperature

The micrograph of the tensile test at RT are shown in Fig. 8. The fractured surface was coated in gold particles prior to viewing to assist in conducting the electron particles. As previously discussed, the mechanical characteristics of SMEP at RT display a ductile property. This can be seen from Fig. 8 (a) and (b) where a riverbed-like pattern fracture surface was observed, indicating that yielding occurred before the sample failed. The rough surface was due to the crack propagation process that occurred before the sample failed. This explains the ductile behavior of the Neat SMEP at RT as discussed before. Fig. 8 (c), (d), and (e) show the fracture surface micrograph

of 3MT 1.0NT with increasing magnifications sequentially. As shown in Fig. 8 (c), the hybrid nanofillers were seen to form the agglomerate indicated by the bright white spots on the surface. Although it was highly difficult to prevent the agglomeration due to the long curing time, the average size of the agglomerate was found to be less than  $5\mu$  and uniformly distributed. This is also attributed to the fact that the fillers interact with each other providing synergetic reinforcement at each site. This can be seen from Fig. 8 (e) where individual MWCNT are found to be protruding from the layer of nanoclay cluster and the epoxy matrix. This shows that the polymer matrix interacts well with the MWCNT surface at a nanometer scale due to the high electrostatic and Van der Waals forces which result in a high interfacial shear strength of about an order of magnitude higher than the nanocomposite itself [81].

On the other hand, Fig. 8 (f) shows the fractured surface of 5MT 1.0NT with a large number of agglomerates of individual nanofillers. This can be seen from Fig. 8 (g), (h), and (i) where large clusters of MWCNT and MMT of more than  $20\mu\text{m}$  respectively were formed consisting of nanofiller of the same type. This indicates a lack of interaction among the nanofillers, thus decreasing the synergetic effect of the nanoparticles towards reinforcement of SMEP nanocomposites. This findings support the results obtained from the RT tensile test discussed previously.

### 3.3.2. High temperature

Fig. 9 shows the micrograph of the fracture surface from the HT tensile test. Referring to Fig. 9 (a) and (b), contradictory to what was observed in the RT tensile test, the fracture surface of Neat SMEP shows a clean fracture surface with sharp edges. Notice the depth of the fracture surface is higher than in Fig. 8 (a) and (b); this is an indication of a decrease in ductility and an inclination towards brittle failure type which was experienced by the SMEP at an elevated temperature. Fig. 9 (c), (d), and (e) show the FESEM image of 1MT 0.5NT in increasing magnifications sequentially. The white dots in Fig. 9 (c) illustrate the state of dispersion of MMT and MWCNT on the fractured surface. The particle showed a good dispersed level; however, Fig. 9 (d) shows that the nanoparticles appeared to be disassociated from each other, indicating a lack of interaction between MMT and MWCNT. This explains the inferior tensile performance as compared to 3MT 1.0NT.

The micrograph of 3MT 1.0NT's fractured surface at an elevated temperature are shown in Fig. 9 (f), (g), and (h) in increasing magnifications sequentially. The micrograph in Fig. 9 (f) shows an increasing number of white dots appear and are dispersed well compared to 1MT 0.5NT in Fig. 9 (c). This indicates a higher reinforcement effect which contributes to a better performance, given that the MMT and MWCNT are well dispersed within the polymer matrix. In addition to a better filler interaction shown in Fig. 8 (e), Fig. 9 (h) displays a good adhesion between the MWCNT and epoxy matrix as all the nanotubes including the agglomerated MWCNT are well covered by the polymer matrix, resulting in a superior mechanical performance.

## 4. Conclusion and recommendation

This study investigate the effects of MWCNT and MMT loading on the mechanical properties of SMEP nanocomposite. It can be concluded that:

- SMEP nanocomposites are ductile at RT where the materials yield before breaking.
- SMEP nanocomposites exhibit a brittle behavior at HT where the material breaks upon reaching UTS.
- Hybrid of 3wt% MMT and 1.0wt% MWCNT produces the highest UTS among all nanocomposites with a 32.5% improvement as compared to Neat SMEP at RT.
- The trend of UTS in HT tensile test shows similar behavior compared to RT tensile test even though the values obtained were a few magnitude lower.
- The flexural test at RT shows an increasing performance with respect to increasing filler loading up to 3wt% MMT and 1.0 wt% MWCNT, and then decreases as the filler loading increases with 3MT 1.0NT recording an improvement of 176% compared to neat SMEP.
- Inconclusive value for flexural modulus at HT due to oscillating data obtained.

In summary, it can be concluded that the hybrid between 3wt% MMT and 1.0wt% MWCNT produces a better mechanical performance in terms of tensile and flexural compared to other filler loadings. This finding can be used as an initial measure in selecting the optimum filler loading for the hybrid nanocomposite between MMT and MWCNT in shape memory polymer. Further tests can be conducted in terms of thermal and shape memory functionality to obtain deeper understanding of hybrid filler SMEP nanocomposite. The shape memory functional stability and operational fatigue can be analyzed to reveal their potential for various applications such as actuator or morphing application as well as biomedical devices

## Conflicts of interest

The authors declare no conflicts of interest.

## Acknowledgement

This work is supported by UPM under GP-IPS Grant, 9647200. The authors would like to express their gratitude and sincere appreciation to Department of Aerospace Engineering, Faculty of Engineering, Universiti Putra Malaysia, and Laboratory of Biocomposite Technology, Institute of Tropical Forestry and Forest Products (INTROP), Universiti Putra Malaysia (HiCOE), for the close collaboration in this research.

## REFERENCES

- [1] Behl M, Lendlein A. Shape-memory polymers. *Mater Today* 2007;10:20–8, [http://dx.doi.org/10.1016/S1369-7021\(07\)70047-0](http://dx.doi.org/10.1016/S1369-7021(07)70047-0).

- [2] Dietsch B, Tong T. A review - Features and benefits of shape memory polymers (SMPs). *J Adv Mater* 2007.
- [3] Xie T. Recent advances in polymer shape memory. *Polymer (Guildf)* 2011;52:4985–5000, <http://dx.doi.org/10.1016/j.polymer.2011.08.003>.
- [4] Ratna D, Karger-Kocsis J. Recent advances in shape memory polymers and composites: a review. *J Mater Sci* 2008;43:254–69, <http://dx.doi.org/10.1007/s10853-007-2176-7>.
- [5] Leng J, Yu K, Sun J, Liu Y. Deployable morphing structure based on shape memory polymer. *Aircr Eng Aerosp Technol* 2015;87:218–23, <http://dx.doi.org/10.1108/AEAT-06-2013-0118>.
- [6] Liu Y, Du H, Liu L, Leng J. Shape memory polymers and their composites in aerospace applications: a review. *Smart Mater Struct* 2014;23:023001, <http://dx.doi.org/10.1088/0964-1726/23/2/023001>.
- [7] Yu K, Yin W, Liu Y, Leng J. Application of SMP composite in designing a morphing wing. *ICEM 2008* 2009;7375:737560, <http://dx.doi.org/10.1117/12.839363>.
- [8] Baer G, Wilson TS, Matthews DL, Maitland DJ. Shape-memory behavior of thermally stimulated polyurethane for medical applications. *J Appl Polym Sci* 2007;103:3882–92, <http://dx.doi.org/10.1002/app.25567>.
- [9] Xie F, Huang L, Leng J, Liu Y. Thermoset shape memory polymers and their composites. *J Intell Mater Syst Struct* 2016;27:2433–55, <http://dx.doi.org/10.1177/1045389X16634211>.
- [10] Mat Yazik MH, Sultan MT, Shah AU, Norkhairunnisa M. Effect of MWCNT content on thermal and shape memory properties of epoxy nanocomposites as material for morphing wing skin. *J Therm Anal Calorim* 2019;6, <http://dx.doi.org/10.1007/s10973-019-08367-6>.
- [11] Wang W, Liu D, Liu Y, Leng J, Bhattacharyya D. Electrical actuation properties of reduced graphene oxide paper/epoxy-based shape memory composites. *Compos Sci Technol* 2015;106:20–4, <http://dx.doi.org/10.1016/j.compscitech.2014.10.016>.
- [12] Leng JS, Huang WM, Lan X, Liu YJ, Du SY. Significantly reducing electrical resistivity by forming conductive Ni chains in a polyurethane shape-memory polymer/carbon-black composite. *Appl Phys Lett* 2008;92, <http://dx.doi.org/10.1063/1.2931049>.
- [13] Lendlein A, Jiang H, Junger O, Langer R. Light-induced shape-memory polymers. *Nature* 2005;434:879–82, <http://dx.doi.org/10.1038/nature03438.1>.
- [14] Yu K, Liu Y, Leng J. Shape memory polymer/CNT composites and their microwave induced shape memory behaviors. *RSC Adv* 2014;4:2961–8, <http://dx.doi.org/10.1039/C3RA43258K>.
- [15] Lv H, Leng J, Liu Y, Du S. Shape-memory polymer in response to solution. *Adv Eng Mater* 2008;10:592–5, <http://dx.doi.org/10.1002/adem.200800002>.
- [16] Schmidt C, Chowdhury AMS, Neuking K, Eggeler G. Thermo-mechanical behaviour of shape Memory Polymers, e.g., Tecoflex by 1WE method: SEM and IR analysis. *J Polym Res* 2011;18:1807–12, <http://dx.doi.org/10.1007/s10965-011-9587-5>.
- [17] Park JH, Dao TD, Lee H II, Jeong HM, Kim BK. Properties of graphene/shape memory thermoplastic polyurethane composites actuating by various methods. *Materials (Basel)* 2014;7:1520–38, <http://dx.doi.org/10.3390/ma7031520>.
- [18] Scott Gibson Rauscher MS, Clark DW. Testing and analysis of shape-memory polymers for morphing aircraft skin application; 2008.
- [19] Williams T, Meador M, Miller S, Scheiman D. Effect of graphene addition on shape memory behavior of epoxy resins. *Soc Adv Mater Process Eng* 2011:1–9.
- [20] Abdullah SA, Jumahat A, Abdullah NR, Frormann L. Determination of shape fixity and shape recovery rate of carbon nanotube-filled shape memory polymer nanocomposites. *Procedia Eng* 2012, <http://dx.doi.org/10.1016/j.proeng.2012.07.362>.
- [21] Liu T, Zhou T, Yao Y, Zhang F, Liu L, Liu Y, et al. Stimulus methods of multi-functional shape memory polymer nanocomposites: a review. *Compos Part A Appl Sci Manuf* 2017;100:20–30, <http://dx.doi.org/10.1016/j.compositesa.2017.04.022>.
- [22] Sun L, Huang WM, Ding Z, Zhao Y, Wang CC, Purnawali H, et al. Stimulus-responsive shape memory materials: a review. *Mater Des* 2012;33:577–640, <http://dx.doi.org/10.1016/j.matdes.2011.04.065>.
- [23] Kumar S, Pandya MV. Thermally recoverable crosslinked polyethylene. *J Appl Polym Sci* 1997, doi:10.1002/(sici)1097-4628(19970502)64:5<823::aid-app1>3.3.co;2-u.
- [24] Jung YC, Yoo HJ, Kim YA, Cho JW, Endo M. Electroactive shape memory performance of polyurethane composite having homogeneously dispersed and covalently crosslinked carbon nanotubes. *Carbon N Y* 2010;48:1598–603, <http://dx.doi.org/10.1016/j.carbon.2009.12.058>.
- [25] Li F, Zhu W, Zhang X, Zhao C, Xu M. Shape memory effect of ethylene-vinyl acetate copolymers. *J Appl Polym Sci* 1999, doi:10.1002/(sici)1097-4628(19990214)71:7<1063::aid-app4>3.3.co;2-1.
- [26] Xu B, Fu YQ, Ahmad M, Luo JK, Huang WM, Kraft A, et al. Thermo-mechanical properties of polystyrene-based shape memory nanocomposites. *J Mater Chem* 2010;20:3442–8, <http://dx.doi.org/10.1039/b923238a>.
- [27] Keihl MM, Bortolin RS, Sanders B, Joshi S, Tidwell Z. Mechanical properties of shape memory polymers for morphing aircraft applications. *Proc SPIE Int Soc Opt Eng* 2005;5762:143–51, <http://dx.doi.org/10.1117/12.600569>.
- [28] Bortolin RS. Characterization of shape memory polymers for use as a morphing aircraft skin material. *Univ Dayt*; 2005.
- [29] Wang M, Zhang L. Recovery as a measure of oriented crystalline structure in poly (ether ester) s based on poly (ethylene oxide) and poly (ethylene terephthalate) used as shape memory polymers. *J Polym Sci Part B: Polym Phys* 1999;37:101–12.
- [30] Park C, Yul Lee J, Chul Chun B, Chung Y, Whan Cho J, Gyoo Cho B. Shape memory effect of poly (ethylene terephthalate) and poly (ethylene glycol) copolymer cross-linked with glycerol and sulfoisophthalate group and its application to impact-absorbing composite material. *J Appl Polym Sci* 2004;94:308–16.
- [31] Yakacki CM, Shandas R, Lanning C, Gall K. Free recovery effects of shape-memory polymers for cardiovascular stents. *MRS Online Proc Libr Arch* 2005;898.
- [32] Santhosh Kumar KS, Biju R, Reghunadhan Nair CP. Progress in shape memory epoxy resins. *React Funct Polym* 2013;73:421–30, <http://dx.doi.org/10.1016/j.reactfunctpolym.2012.06.009>.
- [33] Karger-Kocsis J, Kéki S. Recent advances in shape memory epoxy resins and composites. *Multi-Functionality Polym. Compos* 2015:822–41, <http://dx.doi.org/10.1016/B978-0-323-26434-1.00027-1>.
- [34] Rousseau IA, Xie T. Shape memory epoxy: composition, structure, properties and shape memory performances. *J Mater Chem* 2010;20:3431, <http://dx.doi.org/10.1039/b923394f>.
- [35] Xie T, Rodak DE, Rodgers WR. US 8,618,238 B2 United States patent shape memory epoxy polymers; 2013, <http://dx.doi.org/10.1016/j.73>.
- [36] Xie T, Rousseau IA. Facile tailoring of thermal transition temperatures of epoxy shape memory polymers. *Polymer*

- (Guildf) 2009;50:1852–6, <http://dx.doi.org/10.1016/j.polymer.2009.02.035>.
- [37] Xie T, Daniel E, Rodgers WR. US 20080262188 A1 United States patent shape memory epoxy polymers; 2008.
- [38] Liu Y, Han C, Tan H, Du X. Thermal, mechanical and shape memory properties of shape memory epoxy resin. *Mater Sci Eng A* 2010;527:2510–4, <http://dx.doi.org/10.1016/j.msea.2009.12.014>.
- [39] Feldkamp DM, Rousseau IA. Effect of chemical composition on the deformability of shape-memory epoxies. *Macromol Mater Eng* 2011;296:1128–41, <http://dx.doi.org/10.1002/mame.201100066>.
- [40] Wei K, Zhu G, Tang Y, Tian G, Xie J. Thermomechanical properties of shape-memory hydro-epoxy resin. *Smart Mater Struct* 2012;21, <http://dx.doi.org/10.1088/0964-1726/21/5/055022>.
- [41] Karger-Kocsis J, Kéki S. Review of progress in shape memory epoxies and their composites. *Polymers (Basel)* 2017;10:1–38, <http://dx.doi.org/10.3390/polym10010034>.
- [42] Gunes IS, Cao F, Jana SC. Evaluation of nanoparticulate fillers for development of shape memory polyurethane nanocomposites. *Polymer (Guildf)* 2008;49:2223–34, <http://dx.doi.org/10.1016/j.polymer.2008.03.021>.
- [43] Gunes IS, Jana SC. Shape memory polymers and their nanocomposites: a review of science and technology of new multifunctional materials. *J Nanosci Nanotechnol* 2008;8:1616–37, <http://dx.doi.org/10.1166/jnn.2008.038>.
- [44] Zare Y, Rhee KY. Tensile modulus prediction of carbon nanotubes-reinforced nanocomposites by a combined model for dispersion and networking of nanoparticles. *J Mater Res Technol* 2019;9:22–32, <http://dx.doi.org/10.1016/j.jmrt.2019.10.025>.
- [45] Mu T, Liu L, Lan X, Liu Y, Leng J. Shape memory polymers for composites. *Compos Sci Technol* 2018;160:169–98, <http://dx.doi.org/10.1016/j.compscitech.2018.03.018>.
- [46] Wang W, Liu Y, Leng J. Recent developments in shape memory polymer nanocomposites: actuation methods and mechanisms. *Coord Chem Rev* 2016;320–321:38–52, <http://dx.doi.org/10.1016/j.ccr.2016.03.007>.
- [47] Feng X, Zhang G, Zhuo S, Jiang H, Shi J, Li F, et al. Dual responsive shape memory polymer/clay nanocomposites. *Compos Sci Technol* 2016;129:53–60, <http://dx.doi.org/10.1016/j.compscitech.2016.04.008>.
- [48] Wang Z, Liang Z, Wang B, Zhang C, Kramer L. Processing and property investigation of single-walled carbon nanotube (SWNT) buckypaper/epoxy resin matrix nanocomposites. *Compos Part A Appl Sci Manuf* 2004;35:1225–32, <http://dx.doi.org/10.1016/j.compositesa.2003.09.029>.
- [49] Gardea F, Lagoudas DC. Characterization of electrical and thermal properties of carbon nanotube/epoxy composites. *Compos Part B Eng* 2014;56:611–20, <http://dx.doi.org/10.1016/j.compositesb.2013.08.032>.
- [50] Biercuk MJ, Llaguno MC, Radosavljevic M, Hyun JK, Johnson AT, Fischer JE. Carbon nanotube composites for thermal management. *Appl Phys Lett* 2002;80:2767–9, <http://dx.doi.org/10.1063/1.1469696>.
- [51] Iijima S. Helical microtubules of graphitic carbon. *Nat Publ Gr* 1991, <http://dx.doi.org/10.1038/354056a0>.
- [52] Iijima S, Ichihashi T. Single-shell carbon nanotubes of 1nm diameter. *Nature* 1993;363:603–5.
- [53] Li Y, Huang X, Zeng L, Li R, Tian H, Fu X, et al. A review of the electrical and mechanical properties of carbon nanofiller-reinforced polymer composites. *J Mater Sci* 2019;54:1036–76, <http://dx.doi.org/10.1007/s10853-018-3006-9>.
- [54] Kausar A, Rafique I, Muhammad B. Review of applications of Polymer/Carbon nanotubes and Epoxy/CNT composites. *Polym - Plast Technol Eng* 2016;55:1167–91, <http://dx.doi.org/10.1080/03602559.2016.1163588>.
- [55] Zhang JXJ, Hoshino K. Electrical transducers. *Mol Sensors Nanodevices* 2014:169–232, <http://dx.doi.org/10.1016/b978-1-4557-7631-3.00004-1>.
- [56] Wang Y, Gao X, Wu X, Luo C. Facile synthesis of Mn<sub>3</sub>O<sub>4</sub> hollow polyhedron wrapped by multiwalled carbon nanotubes as a high-efficiency microwave absorber. *Ceram Int* 2020;46:1560–8, <http://dx.doi.org/10.1016/j.ceramint.2019.09.124>.
- [57] Zare Y, Rhee KY. A multistep methodology for calculation of the tensile modulus in polymer/carbon nanotube nanocomposites above the percolation threshold based on the modified rule of mixtures. *RSC Adv* 2018;8:30986–93, <http://dx.doi.org/10.1039/C8RA04992K>.
- [58] Barmar M, Barikani M, Fereidounnia M. Study of polyurethane/clay nanocomposites produced via melt intercalation method. *Iran Polym J (English Ed)* 2006;15:709–14.
- [59] Lakshmi MS, Narmadha B, Reddy BSR. Enhanced thermal stability and structural characteristics of different MMT-Clay/epoxy-nanocomposite materials. *Polym Degrad Stab* 2008;93:201–13, <http://dx.doi.org/10.1016/j.polymdegradstab.2007.10.005>.
- [60] Alexandre M, Dubois P. Polymer-layered silicate nanocomposites: preparation, properties and uses of a new class of materials. *Mater Sci Eng R Rep* 2000;28:1–63, [http://dx.doi.org/10.1016/S0927-796X\(00\)00012-7](http://dx.doi.org/10.1016/S0927-796X(00)00012-7).
- [61] Kojima Y, Usuki A, Kawasumi M, Okada A, Kurauchi T, Kamigaito O. One-pot synthesis of nylon 6-clay hybrid. *J Polym Sci Part A: Polym Chem* 1993;31:1755–8, <http://dx.doi.org/10.1002/pola.1993.080310714>.
- [62] Okada A, Usuki A. The chemistry of polymer-clay hybrids. *Mater Sci Eng C* 1995;3:109–15, [http://dx.doi.org/10.1016/0928-4931\(95\)00110-7](http://dx.doi.org/10.1016/0928-4931(95)00110-7).
- [63] Tang C, Long G, Hu X, Wong KW, Lau WM, Fan M, et al. Conductive polymer nanocomposites with hierarchical multi-scale structures via self-assembly of carbon-nanotubes on graphene on polymer-microspheres. *Nanoscale* 2014;6:7877–88, <http://dx.doi.org/10.1039/c3nr06056j>.
- [64] Zare Y. Modeling approach for tensile strength of interphase layers in polymer nanocomposites. *J Colloid Interface Sci* 2016;471:89–93, <http://dx.doi.org/10.1016/j.jcis.2016.03.029>.
- [65] Wan C, Chen B. Reinforcement and interphase of polymer/graphene oxide nanocomposites. *J Mater Chem* 2012;22:3637–46.
- [66] Sun D, Chu CC, Sue HJ. Simple approach for preparation of epoxy hybrid nanocomposites based on carbon nanotubes and a model clay. *Chem Mater* 2010;22:3773–8, <http://dx.doi.org/10.1021/cm1009306>.
- [67] Zhao Y-Q, Lau K-T, Wang Z, Wang Z-C, Cheung H-Y, Yang Z, et al. Fabrication and properties of clay-supported carbon Nanotube/Poly (vinyl alcohol) nanocomposites. *Polym Compos* 2009;30:702–7, <http://dx.doi.org/10.1002/pc>.
- [68] Kim HS, Kwon H, Kwon SM, Yun YS, Yoon JS, Jin HJ. Electrical and mechanical properties of poly(L-lactide)/carbon nanotubes/clay nanocomposites. *J Nanosci Nanotechnol* 2010;10:3576–80, <http://dx.doi.org/10.1166/jnn.2010.2233>.
- [69] Ayatollahi M, Shokrieh MM, Shadlou S, Kefayati A, Chitsazzadeh M. Mechanical and electrical properties of epoxy/multi-walled carbon nanotube/nanoclay nanocomposites. *Iran Polym J Polym J* 2011:835–43.
- [70] Tüzemen MC, Salıncı E, Avcı A. Enhancing mechanical properties of bolted carbon/epoxy nanocomposites with carbon nanotube, nanoclay, and hybrid loading. *Compos*

- Part B Eng 2017;128:146–54, <http://dx.doi.org/10.1016/j.compositesb.2017.07.001>.
- [71] Hosur M, Mahdi TH, Islam ME, Jeelani S. Mechanical and viscoelastic properties of epoxy nanocomposites reinforced with carbon nanotubes, nanoclay, and binary nanoparticles. *J Reinf Plast Compos* 2017, <http://dx.doi.org/10.1177/0731684417691365>.
- [72] Zeng S, Shen M, Yang L, Xue Y, Lu F, Chen S. Self-assembled montmorillonite–carbon nanotube for epoxy composites with superior mechanical and thermal properties. *Compos Sci Technol* 2018, <http://dx.doi.org/10.1016/j.compscitech.2018.04.035>.
- [73] Lendlein A, Kelch S. Shape-Memory effect from permanent shape. *Angew Chemie* 2002;41:2034–57.
- [74] Zabihi O, Ahmadi M, Nikafshar S, Chandrakumar Preyeswary K, Naebe M. A technical review on epoxy-clay nanocomposites: structure, properties, and their applications in fiber reinforced composites. *Compos Part B Eng* 2017;135, <http://dx.doi.org/10.1016/j.compositesb.2017.09.066>.
- [75] Montazeri A, Montazeri N, Pourshamsian K, Tcharkhtchi A. The effect of sonication time and dispersing medium on the mechanical properties of multiwalled carbon nanotube (MWCNT)/epoxy composite. *Int J Polym Anal Charact* 2011;16:465–76, <http://dx.doi.org/10.1080/1023666X.2011.600517>.
- [76] ASTM. D 638 standard test method for tensile properties of plastics. *Annu Book ASTM Stand Sect 11 Water Environ Technol* 2014;08:1–16, <http://dx.doi.org/10.1520/D0638-10.1>.
- [77] ASTM. D 790 standard test method for flexural properties of unreinforced and reinforced plastics and electrical insulation materials. *Annu Book ASTM Stand Sect 11 Water Environ Technol* 2015:1–11.
- [78] Saba N, Jawaid M, Sultan MTH. An overview of mechanical and physical testing of composite materials. *Mech. Phys. Test. biocomposites, fibre-reinforced compos. Hybrid Compos.*, Elsevier; 2019. p. 1–12.
- [79] McKen LW. 1-Introduction to plastics, polymers, and their properties,”. *Eff. Temp. Other Factors Plast. elastomers*, William Andrew Publishing Oxford, UK; 2014. p. 1–45, <http://dx.doi.org/10.1016/B978-0-323-31016-1.00001-5>.
- [80] Peng W, Rhim S, Zare Y, Rhee KY. Effect of “Z” factor for strength of interphase layers on the tensile strength of polymer nanocomposites. *Polym Compos* 2019;40:1117–22, <http://dx.doi.org/10.1002/pc.24813>.
- [81] Wong M, Paramsothy M, Xu XJ, Ren Y, Li S, Liao K. Physical interactions at carbon nanotube-polymer interface. *Polymer (Guildf)* 2003;44:7757–64, <http://dx.doi.org/10.1016/j.polymer.2003.10.011>.
- [82] Ismail KI, Sultan MTH, Shah AUM, Ariffin AH. Tensile Properties of Hybrid Biocomposite Reinforced Epoxy Modified with Carbon Nanotube (CNT). *BioResources* 2018;13:1787–800.
- [83] Saba N, Safwan A, Sanyang ML, Mohammad F, Pervaiz M, Jawaid M, et al. Thermal and dynamic mechanical properties of cellulose nanofibers reinforced epoxy composites. *Int J Biol Macromol* 2017;102:822–8, <http://dx.doi.org/10.1016/j.ijbiomac.2017.04.074>.
- [84] Liu C, Qin H, Mather PT. Review of progress in shape-memory polymers. *J Mater Chem* 2007;17:1543, <http://dx.doi.org/10.1039/b615954k>.
- [85] Tung WS, Composto RJ, Clarke N, Winey KI. Anisotropic polymer conformations in aligned SWCNT/PS nanocomposites. *ACS Macro Lett* 2015;4:916–20, <http://dx.doi.org/10.1021/acsmacrolett.5b00256>.
- [86] Pothan LA, Thomas S, Groeninckx G. The role of fibre/matrix interactions on the dynamic mechanical properties of chemically modified banana fibre/polyester composites. *Compos Part A Appl Sci Manuf* 2006;37:1260–9, <http://dx.doi.org/10.1016/j.compositesa.2005.09.001>.
- [87] Laoubi K, Hamadi Z, Benyahia AA, Serier A, Azari Z. Thermal behavior of E-glass fiber-reinforced unsaturated polyester composites. *Compos Part B Eng* 2014;56:520–6.
- [88] Ridzuan MJM, Majid MSA, Afendi M, Mazlee MN, Gibson AG. Thermal behaviour and dynamic mechanical analysis of Pennisetum purpureum/glass-reinforced epoxy hybrid composites. *Compos Struct* 2016;152:850–9, <http://dx.doi.org/10.1016/j.compstruct.2016.06.026>.
- [89] Thill C, Etches J, Bond I, Potter K, Weaver P. Morphing skins. *Aeronaut J* 2008;112:117–39, doi:3216.
- [90] Gross KE. Mechanical characterization of shape memory polymers to assess candidacy As morphing aircraft skin; 2008.
- [91] Azmi AMR, Sultan MTH, Jawaid M, Talib ARA, Nor AFM. Tensile and flexural properties of a newly developed bulletproof vest using a Kenaf/X-ray film. *Hybrid Composite* 2018;13:4416–27.
- [92] Zhou Y, Pervin F, Lewis L, Jeelani S. Experimental study on the thermal and mechanical properties of multi-walled carbon nanotube-reinforced epoxy. *Mater Sci Eng A* 2007;452–453:657–64, <http://dx.doi.org/10.1016/j.msea.2006.11.066>.
- [93] Chen W, Auad ML, Williams RJJ, Nutt SR. Improving the dispersion and flexural strength of multiwalled carbon nanotubes–stiff epoxy composites through  $\beta$ -hydroxyester surface functionalization coupled with the anionic homopolymerization of the epoxy matrix. *Eur Polym J* 2006;42:2765–72.
- [94] Zare Y, Rhee KY, Park SJ. A modeling methodology to investigate the effect of interfacial adhesion on the yield strength of MMT reinforced nanocomposites. *J Ind Eng Chem* 2019;69:331–7, <http://dx.doi.org/10.1016/j.jiec.2018.09.039>.
- [95] Loos MR, Manas-Zloczower I. Reinforcement efficiency of carbon nanotubes-myth and reality. *Carbon Nanotub Reinf Compos CNR Polym Sci Technol* 2014:233–46, <http://dx.doi.org/10.1016/B978-1-4557-3195-4.00009-6>.
- [96] Hadavand BS, Javid KM, Gharagozlou M. Mechanical properties of multi-walled carbon nanotube/epoxy polysulfide nanocomposite. *Mater Des* 2013;50:62–7.
- [97] Nor AFM, Sultan MTH, Jawaid M, Abu Talib AR, Azmi AMR, Harmaen AS, et al. The effects of multi-walled CNT in Bamboo/Glass fibre hybrid composites: tensile and flexural properties. *BioResources* 2018;13:4404–15.
- [98] Gross KE, Weiland L. Flexural testing of shape memory polymers for morphing aircraft applications. *ASME Conf Proc* 2007;2007:299–303, <http://dx.doi.org/10.1115/IMECE2007-43219>.
- [99] Ramli WMAW, Ridzuan MJM, Majid MSA, Rahman YMN, Azduwin K. Effect of elevated temperatures on flexural strength of hybrid Napier / glass reinforced epoxy composites Effect of elevated temperatures on flexural strength of hybrid Napier / glass reinforced epoxy composites. *J Phys Conf Ser* 2017.
- [100] Lu H, Yu K, Sun S, Liu Y, Leng J. Mechanical and shape-memory behavior of shape-memory polymer composites with hybrid fillers. *Polym Int* 2010;59:766–71, <http://dx.doi.org/10.1002/pi.2785>.